Two-parameter study of ^{236}U fission using thin-film scintillation detectors

N. N. Ajitanand, K. N. Iyengar, and S. R. S. Murthy
Nuclear Physics Division, Bhabha Atomic Research Centre, Trombay, Bombay, India 400 085
(Received 30 December 1977)

A new technique involving detection of both fragments associated with each fission event by two thin-film scintillation detectors is investigated to obtain information about fragment mass and energy. The functional behavior of the film response to fission fragments of specified E/M and Z is obtained by combining the specific luminescence and specific energy loss data for heavy ions. The analysis of the scintillation data gives fragment mass and energy distributions and mass-energy correlations whose main features are in good agreement with those of semiconductor detector measurements. In addition it is found that the scintillation data are capable of revealing information on the average charge to mass relation of the fragments in the symmetric region.

[NUCLEAR REACTIONS, FISSION Fragment mass-energy investigation with thin-film scintillation detectors.]

INTRODUCTION

The development of the thin-film scintillation detector (TFSD) has gained considerable importance because of its obvious applications in the study of heavy-ion reactions and fission phenomena. It has an advantage over the more commonly used solid-state detector in its ability to withstand heavy doses of charged particles without showing any appreciable deterioration in response. Several techniques of TFSD preparation have been reported[1-3] and models[4,5] have been proposed to give a description of the experimentally observed specific luminescence due to various heavy ions.

There are certain advantages in using TFSD's for fission investigations. The detector response does not deteriorate even after receiving large doses of fission fragments, which makes it particularly useful in investigating charged-particle induced fission and rare phenomena such as light charged particles accompanying fission and fission isomers, wherein large doses of charged particles may have to be received by the detector. The fast response (rise time ~2 nsec) can be used advantageously in fast coincidence experiments and time-of-flight applications.

With a view to testing the applicability of the TFSD in fission studies, we have used two TFSD's in a two-parameter investigation of the thermal-neutron-induced fission of ^{235}U. The data have been analyzed using a parametrized response function for the TFSD in terms of the fragment charge and velocity to obtain the fragment mass and energy distributions and mass-energy correlations. The results obtained compare very favorably with those obtained by using conventional double-energy measurements employing semiconductor detectors.

EXPERIMENT

The experiment was carried out at one of the beam holes of the CIRUS reactor. To reduce the background due to scattered fast neutrons, entrance and exit windows were provided in the experimental chamber for the collimated neutron beam. The thermal neutron flux at the source was about 10^7 cm^{-2} sec^{-1}.

Source

A 60 μg/cm^2 thick ^{235}U source was prepared by the electrospraying technique on a gold coated VYNS plastic film support which degraded the energy of fragments passing normally through it by about 3 MeV. The source was mounted in between the detectors as shown schematically in Fig. 1 so that the source-detector distance on either side was about 4 cm. The quality of the

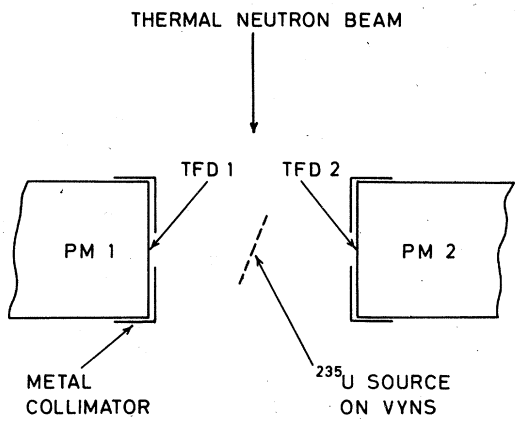

FIG. 1. Schematic diagram of the experimental arrangement.

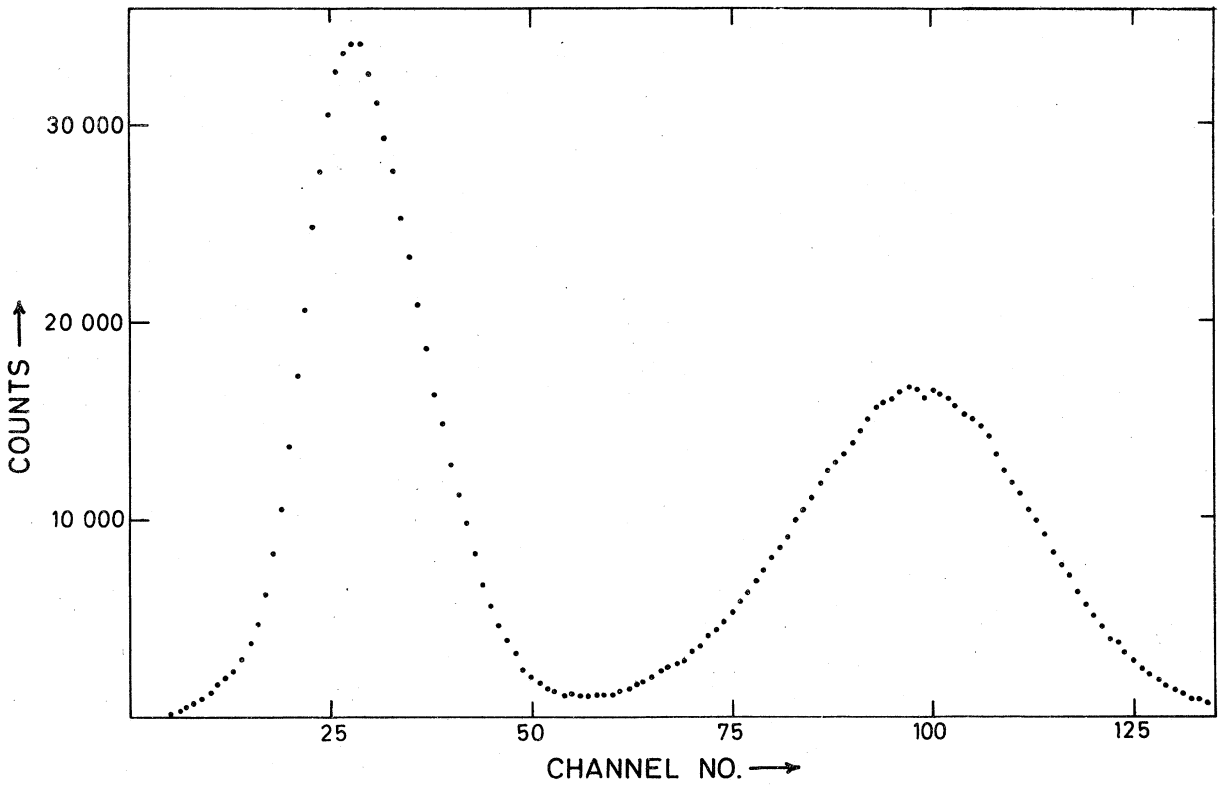

FIG. 2. Coincident single fragment pulse-height distribution from one of the TFSD's.

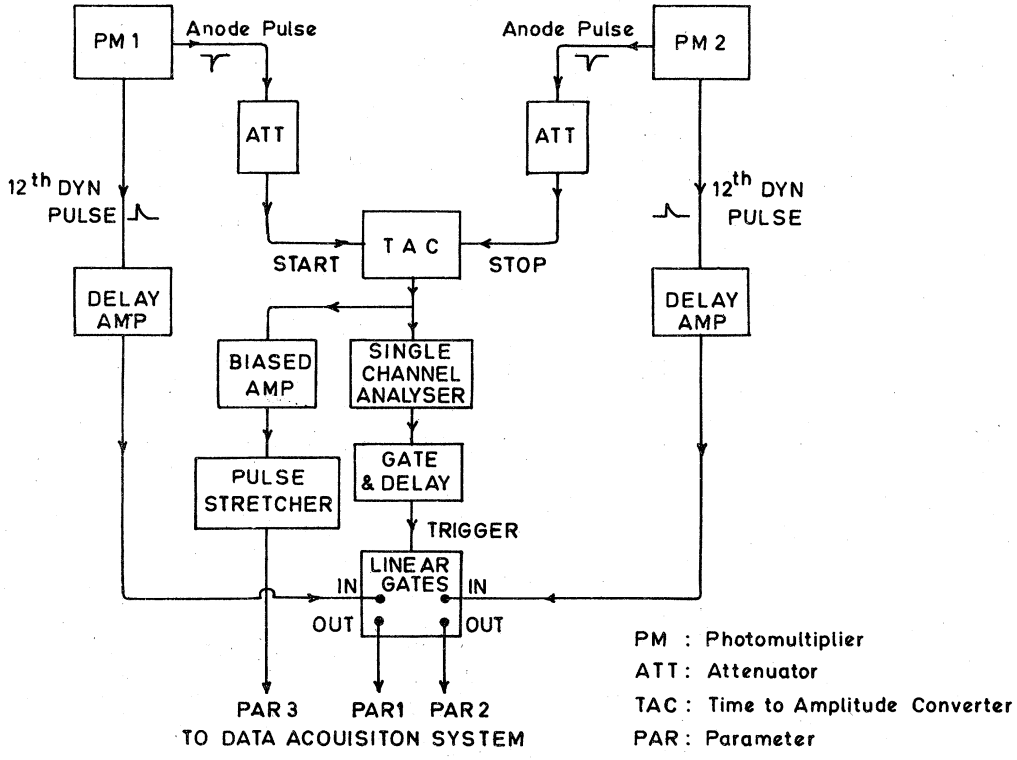

FIG. 3. Block diagram of the electronics.

source was tested by recording the fission fragments with a solid-state detector and observing the peak-to-valley ratio of the pulse-height distribution.

Detectors

The TFSD's were prepared directly on photomultiplier faces from a solution of NE102A in toluene by a technique reported earlier.[6] Each film was about 15 μm thick. Each detector was covered with a metallic collimator to expose only a central portion of 1.5-cm diameter to the source. This ensured that the fragments saw a uniform thickness of the film and also provided an optimum light collection geometry for the photocathode. A typical fission fragment pulse-height distribution from one of these detectors is seen in Fig. 2.

Electronics

The photomultipliers used were RCA 6810A and were operated at 1800-V anode voltage. The fast anode pulses were fed directly to the start and stop inputs of an ORTEC time-to-pulse height converter whose output, together with the 10th dynode outputs of the two photomultipliers, was recorded event-by-event on magnetic tape by a multiparameter data acquisition system. The recorded event rate was about two per second. A block diagram of the electronics used is shown in Fig. 3.

DATA ANALYSIS

TFSD response function

In order to obtain information about fragment mass and energy from the multiparameter data, it was necessary to define a response function for the TFSD in terms of the charge, mass, and energy of the incident heavy ion. The total light output L due to a heavy ion with charge Z, mass M, and energy E incident on a TFSD of thickness T is given by:

$$L_T(Z,E,M) = \int_E^{E'} \frac{dL/dx}{dE/dx} dE , \tag{1}$$

where $(E - E')$ is the energy deposited in the film, dE/dx is the specific energy loss in the film, and dL/dx is the corresponding specific luminescence. To evaluate the above integral, a semiempirical expression for dL/dx based on a new model for luminescence production by charged particles was used which reproduced the experimental data very well.[5] The function chosen to represent dE/dx was a generalized conic section whose parameters were determined using the tabulations of Northcliffe and Schilling.[7] The integration in Eq. (1) was carried out over a range of energies and masses covered by fragments arising in heavy element fission. Some of these results for a TFSD thick enough to completely stop the fragments are shown in Fig. 4. The dependence of

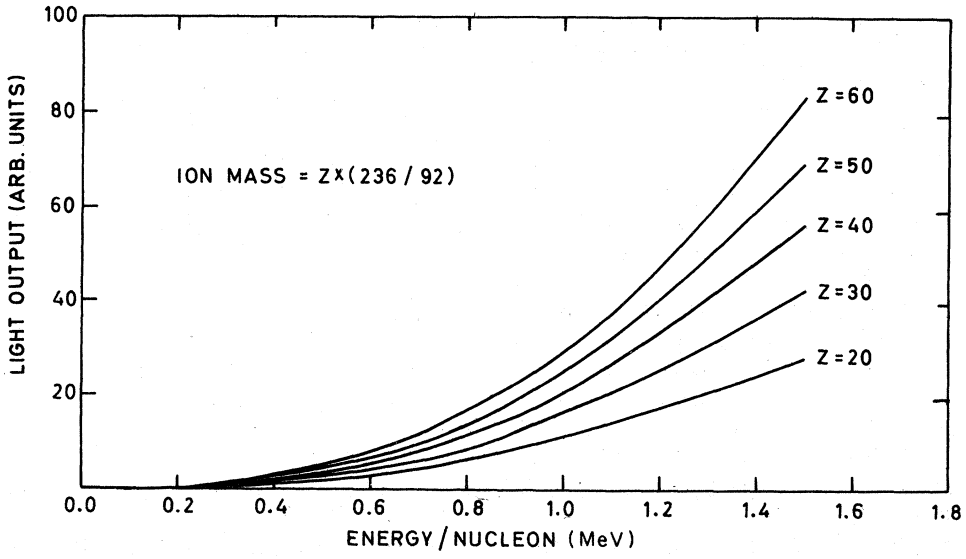

FIG. 4. Calculated TFSD response L vs E/M for fission fragments of different nuclear charge which are completely stopped within the film.

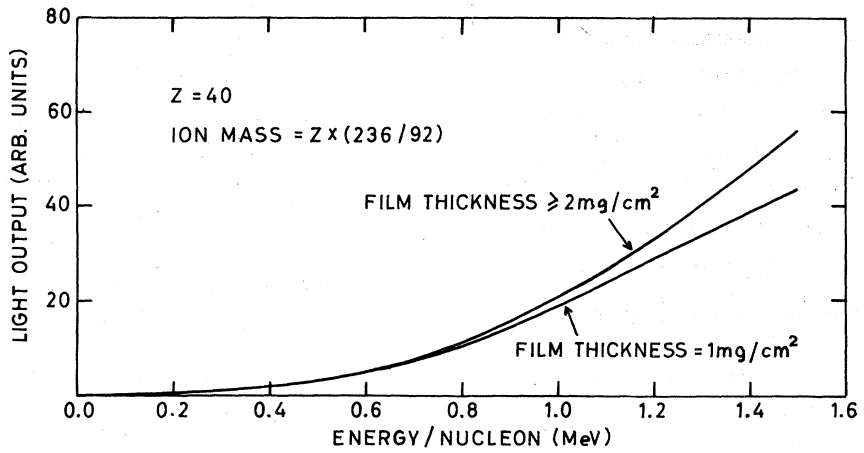

FIG. 5. Calculated TFSD response L vs E/M for $Z = 40$ for different film thicknesses.

these curves on ion mass was found to be negligibly small for variations of five in A about the value given by $M = Z \times (236/92)$. The effect of a smaller film thickness lowers the light output correspondingly, as is seen in Fig. 5. The response curves can be well represented by polynomials of the type

$$L_T = \sum_{i=1}^{5} A_i^T(Z)(E/M)^{i-1},$$

where

$$A_i^T(Z) = \sum_{j=1}^{4} B_{ij}^T Z^{j-1}. \quad (2)$$

The response matrix B_{ij}^T for a TFSD of thickness T thus completely describes its response to fragments of different Z and E/M. The set corresponding to the thickness (~15 μm) of the films employed in the present experiment was calculated and used for fragment mass and energy determinations event-by-event as described in the following section.

Computations

The coincidence time distribution obtained from the time-to-pulse height converter is shown in Fig. 6. It is believed that the double-peaked nature of the distribution shows up strikingly a dependence of the rise time of the anode pulse height on the fragment type, since there is a one-to-one correspondence between the two peaks and the light and heavy peaks of the dynode pulse height distributions. The peaks are separated by approximately 20 nsec, which is too large to be accounted for by the time-of-flight differences between the light and heavy fragments or the pulse-height associated walks of the discriminators. This is a feature of the TFSD which, when properly understood, can be used to obtain more detailed information about the fragments. In the present analysis, no use is made of the time distribution other than to identify time coincidences between correlated fragments.

The dynode pulse-height distributions were calibrated in terms of the light output by associating the two peak positions with the calculated response for the most probable light and heavy fragments with specific Z and E/M after accounting for the energy losses suffered in the source and backing by the fragments. Having calibrated the pulse height distributions of the two TFSD's, the values L_1 and L_2 calculated from the recorded pulse heights for a given fragment pair were used in an iterative calculation to obtain the masses and energies of the fragments under the following necessary and sufficient conditions:

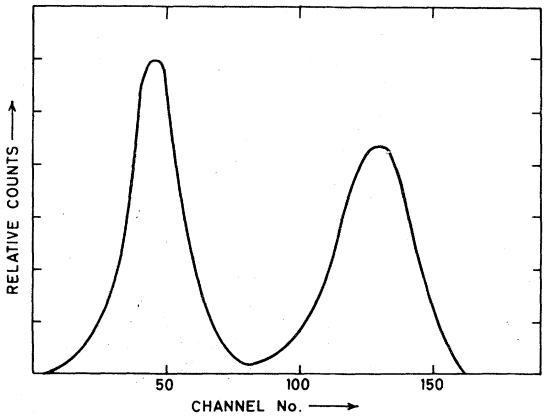

FIG. 6. Double humped time to pulse-height converter output distribution showing evidence for dependence of TFSD pulse rise time on fragment type.

$M_1 + M_2 = 236$ (mass conservation),

$Z_1 + Z_2 = 92$ (charge conservation),

$M_1 E_1 = M_2 E_2$ (momentum conservation),

$(Z_1/M_1) = (Z_2/M_2) = 92/236$

(unchanged charge distribution), (3)

$L_1 = L_1(E_1/M_1, Z_1)$ (from response matrix),

$L_2 = L_2(E_2/M_2, Z_2)$ (from response matrix).

The iteration also incorporated a correction for energy loss of fragment 1 in the source and the VYNS backing, and for fragment 2 in the source only. Since neutron emission from a fragment would not seriously alter its Z and E/M, no correction to the TFSD response for neutron emission effects was included in the calculations.

RESULTS AND DISCUSSION

The mass yield, the width, the average of the total kinetic energy distribution, and the average

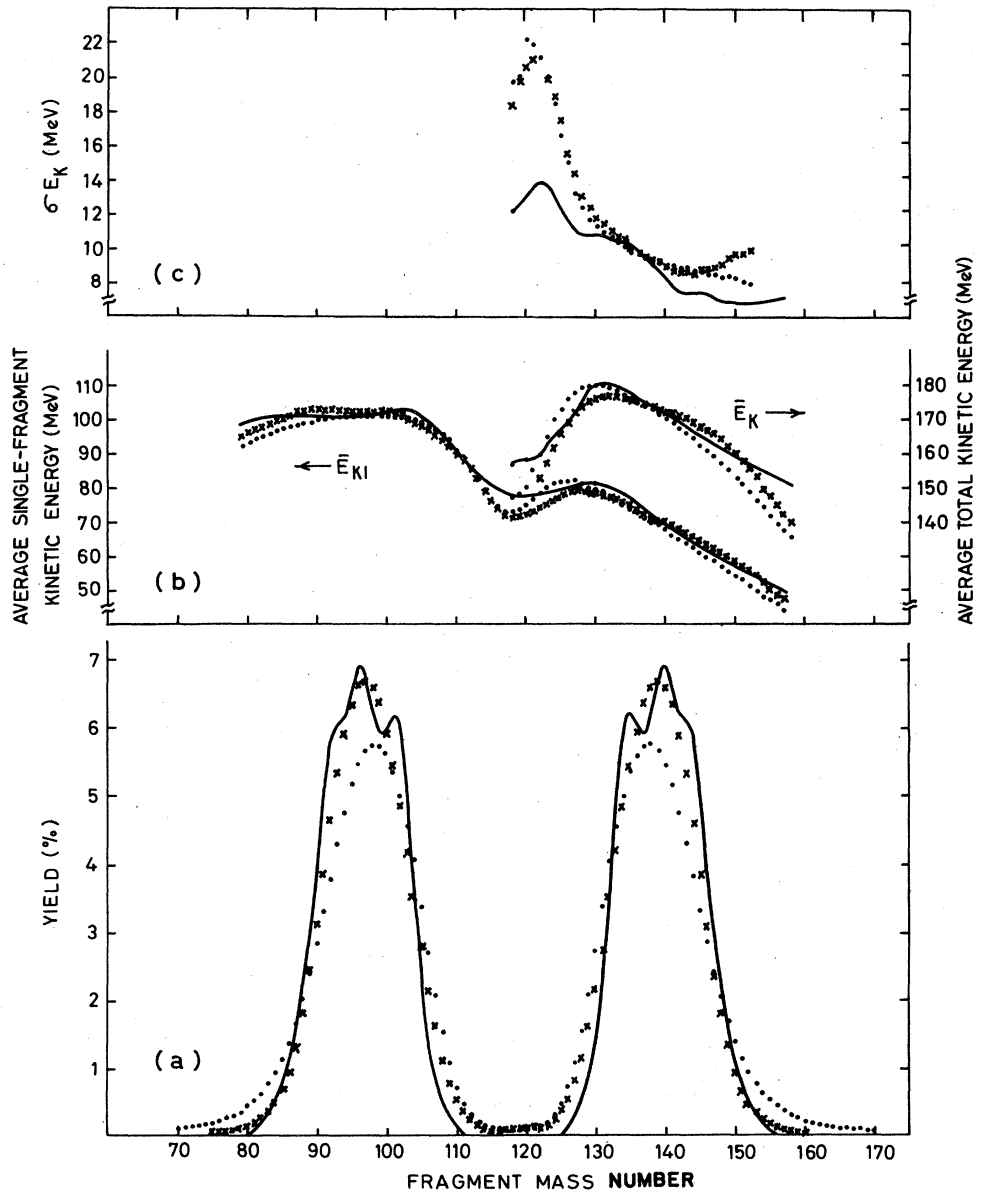

FIG. 7. Results of the TFSD data analysis to obtain (a) fragment mass distribution, (b) average total kinetic energy and average single fragment kinetic energy vs mass, and (c) rms width of total kinetic energy vs mass. Continuous lines show semiconductor results (Ref. 8), closed circles show TFSD results with calculated response functional [Eq. (1)], and crosses show TFSD results with assumed response function [Eq. (4)].

single-fragment kinetic energy as a function of fragment mass obtained from TFSD data are shown as closed circles in Fig. 7. For comparison, the results of the semiconductor detector (SCD) measurements of Schmitt *et al.*[8] are also shown (continuous lines), from which it can be seen that the TFSD technique is able to give results which are in qualitative agreement with those obtained by conventional methods.

In order to see if small changes in the response function would improve the quantitative agreement, the data were analyzed with the response function given by

$$L(E/M,Z) = (a+bZ)(E/M)^c , \qquad (4)$$

for different values of the parameters. The results obtained with $b/a = 0.38$ and $c = 2.1$ are shown as crosses in Fig. 7. The improvement in the agreement between the SCD and TFSD measurements, especially for the mass distribution, is quite considerable. The response functions used for the two analyses are compared in Fig. 8 for typical Z values.

It is seen from Fig. 7 that the peak-to-valley ratio of the mass distribution obtained from the TFSD data is rather small (~60) compared to that of the SCD data (~300). This disagreement persists in spite of considerable variations in the assumed Z dependence (given by b/a) and E/M dependence (given by c) of the TFSD response. However, the calculated mass in the symmetric region was found to be very sensitive to the average charge-mass relation assumed [see Eq. (3)]. It is interesting to note that the charge-mass relation as determined experimentally[9] shows that although in the most probable region the heavy fragment is more neutron rich than the parent nucleus, as one approaches the symmetric region the trend may well be reversed. Unfortunately, because of the low yield, experimental points in the symmetric region have not been obtained. When such a possibility is admitted into the assumed charge-mass relation in Eq. (3), the mass yield obtained from the TFSD data in the symmetric region conforms much more closely with that obtained from solid-state detector data. This is illustrated in Fig. 9 where the calculated mass yield in the symmetric region is shown for different assumptions of the charge-mass relation in the symmetric region.

There are two aspects of the charge-mass relation implied by the present analysis which are worth noting. One is the rather abrupt change in the $(\bar{Z} - Z_{\mathrm{UCD}})$ value as one approaches symmetry, implying an unequal charge division between the two fragments. The resulting smaller Coulomb potential at scission can account to a large extent for the observed dip in the total kinetic energy at symmetry. The occurrence of such a situation may be understood in terms of the Coulomb repulsion between the charge groups in the fissioning nucleus, which increases with the approach to an equal charge division and thus strongly inhibits a further transfer of protons between the two frag-

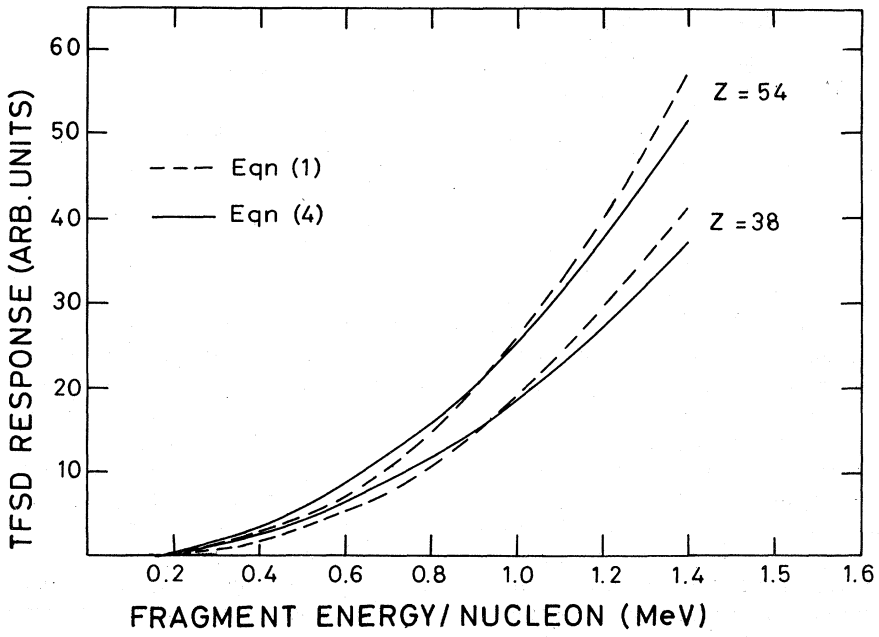

FIG. 8. TFSD response vs E/M computed from Eqs. (1) and (4).

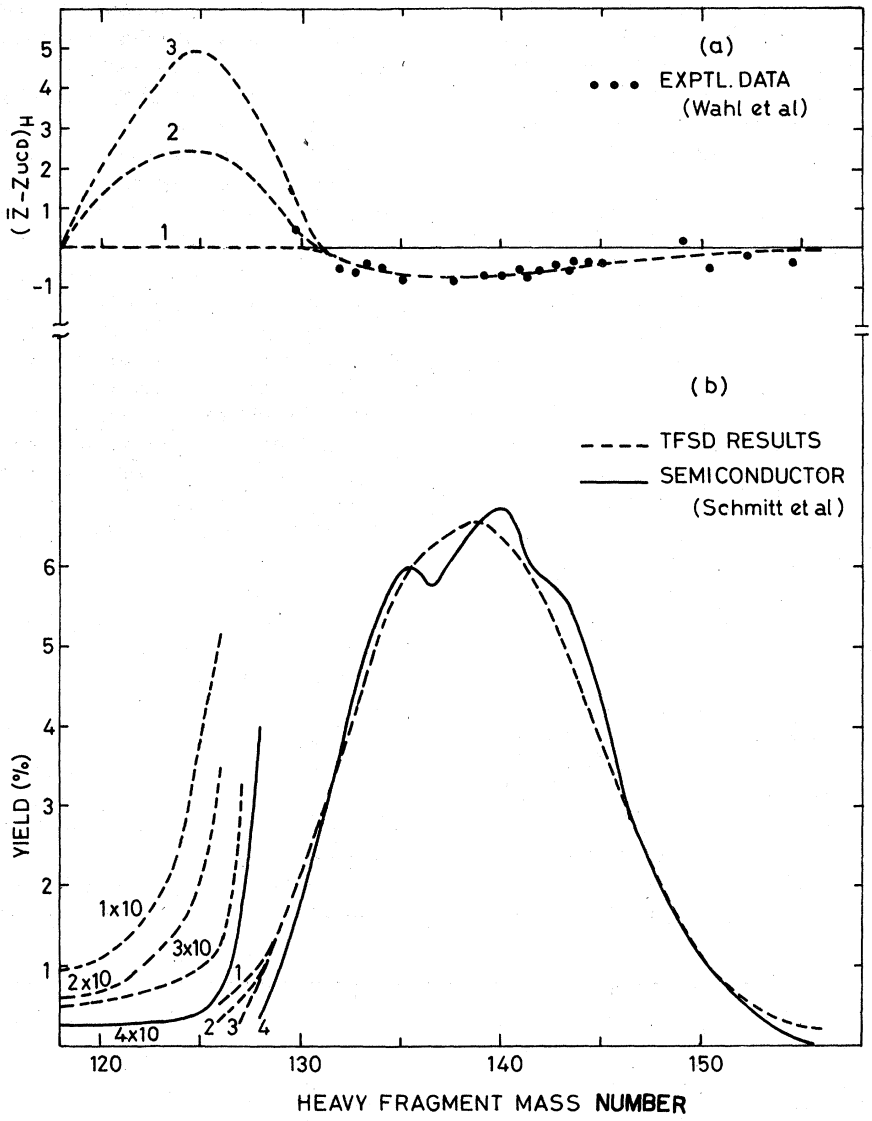

FIG. 9. Fragment mass distributions (b) obtained from TFSD data for different assumptions of the average charge to mass relation (a).

ments prior to scission. No such restriction exists on the transfer of neutrons. Ramanna[10] had postulated several years ago that such nucleon transfers between the two sides of the nucleus during its descent from saddle to scission may well be the governing factor in determining the observed fragment mass yield. The other aspect of the charge-mass relation is the occurrence of the positive values of $\bar{Z}-Z_{UCD}$ in the region around mass 125. This implies a smaller neutron richness of the fragments and hence a smaller yield of evaporated neutrons in this region and a correspondingly larger yield in the complementary light fragment region. Experimental data of Apalin *et al.*[11] on neutron emission from fragments do support this expectation.

It is, of course, not possible to be definite about the actual charge-mass relationship in the symmetric region from this analysis unless one can be sure that the mass dispersion due to detector resolution is not the overriding factor in establishing the shape of the calculated mass yield curve in the symmetric region.

It is obvious that the determination of the response function of the TFSD would be best done by the use of heavy ions of known mass, charge, and energy. An experimentally determined function will be more realistic and may give better

quantitative agreement with the established results when used to analyse the double TFSD data. This will also help in determining the overall mass resolution of this technique. In conclusion, it can be said that the present work has successfully demonstrated the potentialities of the TFSD technique in fission investigations.

The authors are grateful to Dr. S. S. Kapoor for many useful discussions.

[1]M. L. Muga, D. J. Burnsted, and W. E. Steeger, Nucl. Instrum. Methods 104, 605 (1972).
[2]P. D. Goldstone, R. E. Malmin, F. Hopkins, and P. Paul, Nucl. Instrum. Methods 121, 353 (1974).
[3]R. K. Batra and A. C. Shotter, Nucl. Instrum. Methods 124, 101 (1975).
[4]M. L. Muga and M. Diksic, Nucl. Instrum. Methods 122, 553 (1974).
[5]N. N. Ajitanand, Nucl. Instrum. Methods 143, 345 (1977).
[6]N. N. Ajitanand and K. N. Iyengar, Nucl. Instrum. Methods 133, 71 (1976).
[7]L. C. Northcliffe and R. F. Schilling, Nucl. Data A7, 233 (1970).
[8]H. W. Schmitt, J. H. Neiler, and F. S. Walter, Phys. Rev. 141, 1146 (1966).
[9]A. C. Wahl, R. L. Ferguson, D. R. Nethaway, D. E. Troutner, and K. Wolfsberg, Phys. Rev. 126, 1112 (1962).
[10]R. Ramanna, Phys. Lett. 10, 321 (1964).
[11]A. V. F. Apalin, Yu. N. Gritsyuk, T. E. Kutikov, V. I. Lebedev, and L. A. Mikaelyan, in Proceedings of the Symposium on the Physics and Chemistry of Fission, Salzburg, 1965 (International Atomic Energy Agency, Vienna, 1965) 1, 586.